

Reactive Organic Carbon Air Emissions from Mobile Sources in the United States

Benjamin N. Murphy^{1*}, Darrell Sonntag², Karl M. Seltzer³, Havalala O. T. Pye¹, Christine Allen⁴, Evan Murray⁵, Claudia Toro⁵, Drew R. Gentner⁶, Cheng Huang⁷, Shantanu Jathar⁸, Li Li⁶, Andrew A. May⁹, and Allen L. Robinson¹⁰

¹Center for Environmental Measurement and Modeling, US Environmental Protection Agency, Research Triangle Park, North Carolina 27711, United States

²Department of Civil and Construction Engineering, Brigham Young University, Provo, Utah 84602, United States

³Office of Air Quality Planning and Standards, US Environmental Protection Agency, Research Triangle Park, North Carolina 27711, United States

⁴General Dynamics Information Technology, 79 T.W. Alexander Drive, Research Triangle Park, NC 27709, United States

⁵Office of Transportation and Air Quality, US Environmental Protection Agency, Ann Arbor, Michigan 48105, United States

⁶Department of Chemical and Environmental Engineering, Yale University, New Haven, CT 06511, United States

⁷State Environmental Protection Key Laboratory of Cause and Prevention of Urban Air Pollution Complex, Shanghai Academy of Environmental Sciences, Shanghai, 200233, China

⁸Department of Mechanical Engineering, Colorado State University, Fort Collins, Colorado 80523, United States

⁹Department of Civil, Environmental and Geodetic Engineering, The Ohio State University, Columbus, Ohio 43210, United States

¹⁰Department of Mechanical Engineering, Carnegie Mellon University, Pittsburgh, Pennsylvania 15213, United States; Carnegie Mellon University Africa, BP 6150 Kigali, Rwanda

*Correspondence to: Benjamin N. Murphy (murphy.ben@epa.gov)

Abstract: Mobile sources are responsible for a substantial controllable portion of the reactive organic carbon (ROC) emitted to the atmosphere, especially in urban environments of the United States (U.S.). We update existing methods for calculating mobile source organic particle and vapor emissions in the U.S. with over a decade of laboratory data that parameterize the volatility and organic aerosol (OA) potential of emissions from onroad vehicles, nonroad engines, aircraft, marine vessels, and locomotives. We find that existing emission factor information from teflon filters combined with quartz filters collapses into simple relationships and can be used to reconstruct the complete volatility distribution of ROC emissions. This new approach consists of source-specific filter artifact corrections and state-of-the-science speciation including explicit intermediate volatility organic compounds (IVOCs), yielding the first bottom-up volatility-resolved inventory of U.S. mobile source emissions. Using the Community Multiscale Air Quality model, we estimate mobile sources account for 20-25% of the IVOC concentrations and 4.4-21.4% of ambient OA. The updated emissions and air quality model reduce biases in predicting fine-particle organic carbon in winter, spring, and autumn throughout the U.S. (4.3-11.3% reduction in normalized bias). We identify key uncertain parameters that align with current state-of-the-art research measurement challenges.

1. Introduction

Ambient particulate matter (PM) and ozone (O₃) have detrimental impacts on human health and the environment (U.S. Epa, 2019, 2020c; Pye et al., 2021) with disparate impacts across societal groups (Tessum et al., 2021). Non-methane organic gases (NMOG) are precursors to PM and O₃, and reducing NMOG could reduce criteria pollutants and their associated mortality throughout the United States (U.S.) (Pye et al., 2022a). Mobile source emissions continue to be a major contributor to modern anthropogenic NMOG emissions. In contrast to other NMOG sources such as vegetation, mobile emissions have been reduced through successful regulatory policy and the introduction of cleaner engine and control technologies (Lurmann et al., 2015; Gentner et al., 2017; Winkler et al., 2018; Bessagnet et al.,

45 2022). Yet, effective management of urban and regional air quality still depends on accurate and detailed
46 characterization of the carbon-containing compounds emitted by mobile sources.

47 Fossil-fuel combustion emissions comprise thousands of organic compounds with widely varying volatility,
48 depending on source type (Drozd et al., 2018; Lu et al., 2018). The lowest volatility compounds are emitted principally
49 in the particle phase and are typically classified as primary organic aerosol (POA). Conventionally this portion of
50 emissions is sampled using filters which are weighed or processed off-line with thermal-optical techniques, solvent
51 extraction, and other methodologies (Chow et al., 1993; Birch and Cary, 1996; U.S. Epa, 2022c). The highest volatility
52 NMOGs are emitted in the gas-phase and enhance O₃ formation when oxidized in the atmosphere, a process that also
53 enhances PM mass via secondary organic aerosol (SOA) formation. U. S. EPA emission tools like the MOTO Vehicle
54 Emission Simulator (MOVES) (U.S. Epa, 2020b) and the SPECIATE database (U.S. Epa, 2020a) provide emission
55 estimates and speciation for POA (assumed to be nonvolatile) and NMOGs. The ‘Conventional’ path in Fig. 1 depicts
56 this process.

57 However, laboratory and field measurement campaigns have demonstrated that much of the mobile source POA is
58 subject to gas-particle partitioning and filter sampling artifacts. These artifacts may bias the interpretation of filter-
59 based measurements by yielding higher POA emission factors due to the presence of these adsorbed vapors (Turpin
60 et al., 1994; Robinson et al., 2010; Bessagnet et al., 2022). These compounds principally include (Table 1) semivolatile
61 organic compounds (SVOCs) and intermediate volatility organic compounds (IVOCs)(May et al., 2013b, a).
62 Accurately representing SVOCs and IVOCs is important because they are SOA precursors and are underestimated in
63 contemporary models and emission databases (Gentner et al., 2012; Tkacik et al., 2012; Zhao et al., 2014; Zhao et al.,
64 2015, 2016b).

65 Some air quality models (AQMs) have incorporated semivolatile organic compounds (SVOCs) and IVOCs by scaling
66 these emissions to sector-wide POA or NMOG inputs during a data pre-processing step or the AQM runtime (Murphy
67 and Pandis, 2009; Shrivastava et al., 2011; Ahmadov et al., 2012; Bergström et al., 2012; Koo et al., 2014; Woody et
68 al., 2015; Zhao et al., 2016a; Woody et al., 2016; Jathar et al., 2017b; Murphy et al., 2017). However, these approaches
69 rely on broad application of assumptions that may not be appropriate for specific source types since sampling artifacts
70 will bias low-emitting and high-emitting sources differently (Robinson et al., 2010). As emissions from individual
71 combustion sources are continually reduced in response to tightening regulations, accounting for these potential biases
72 becomes important. Bottom-up approaches are needed that revise emission factors and speciation profiles for
73 individual source types. Manavi and Pandis (2022) and Sarica et al. (2023) implement emission factors and speciation
74 of SVOCs and IVOCs specific for mobile sources in Europe, while Morino et al. (2022) explores revisions to
75 stationary source ROC emissions in Japan. Chang et al. (2022) implements a more detailed bottom-up inventory of
76 ROC emissions across all sectors in China with emission factors specified at the volatility bin level rather than for
77 bulk PM and NMOG.

78 This paper documents the transition of U. S. EPA mobile emission tools from the conventional paradigm that considers
79 operationally defined particulate organic matter (OM) and NMOG emission factors and speciation to one that
80 accommodates the full complexity of atmospheric carbon-containing trace pollutants. To accomplish this, we consider

81 total Reactive Organic Carbon (ROC), defined by Saffedine et al. (2017) and Heald and Kroll (2020) as all reactive
82 organic compound mass across gas and particle phases excluding methane. We catalogue updates to 51 diverse mobile
83 source categories across multiple categories and engine, fuel, and control types. Further, we demonstrate procedures
84 for integrating existing inventory emission factors with state-of-the-art chemical composition measurements, pointing
85 out where critical uncertainties could be further resolved in the future. Finally, we document the impact the updates
86 have on source-specific and sector-wide emissions as well as regional-scale pollutant formation and transport
87 predicted by an updated version (2020) of the Community Multiscale Air Quality (CMAQ) regional-scale AQM.

88 **2. Materials and Methods**

89 **2.1 Mobile Emission Modeling**

90 To develop the new framework and estimate potential impacts from speciation updates, we used existing estimates for
91 2016 annual mobile emissions for the contiguous U.S. We considered five categories including onroad, nonroad, air,
92 rail, and marine. The MOVES3 model predicts emissions for onroad and nonroad sources using county-level fleet
93 properties and activity data. The dominant U.S. onroad vehicle sources are light-duty gasoline cars and trucks and
94 heavy-duty diesel trucks. Nonroad emission sources include construction, agricultural, and lawn equipment as well as
95 nonroad recreational vehicles. The Aviation Environmental Design Tool (AEDT), maintained by the Federal Aviation
96 Administration, predicts landing, taxi, and take-off emissions for aircraft and emissions from ground support
97 equipment (FAA, 2022). Rail emissions are calculated using confidential line-haul activity data that were summarized
98 at the county-level, while rail-yard emissions are based on supply fuel use and yard switcher counts provided by
99 companies (U.S. Epa, 2022b). Marine emissions include both port and underway conditions for large, generally
100 international ships, vessels, and smaller boats operating near shore (U.S. Epa, 2022b). The MOVES3 model predicts
101 emissions from recreational boats as part of the nonroad recreational equipment category.

102 We also collected national total annual fuel usage data for each source from the models to calculate an effective fuel-
103 based OM emission factor (see section S1). These effective emission factors range from 1-20 mg (kg-fuel)⁻¹ for the
104 newest gasoline, diesel, and compressed natural gas (CNG) vehicles to over 6000 mg (kg-fuel)⁻¹ for nonroad gasoline
105 two-stroke engines. In the process of reviewing each mobile source OM emission rate, we discovered and corrected
106 several minor errors and limitations to compressed natural gas sources and uncontrolled nonroad diesel exhaust (see
107 section S2).

108 **2.2 Reactive Organic Carbon (ROC)**

109 To accurately simulate the behavior of mobile emissions, we must consider total ROC which includes organic carbon
110 (OC) and non-carbon mass from compounds from the most volatile species like ethane and formaldehyde to
111 chemically complex, high molecular weight compounds (e.g. oligomers) (Heald and Kroll, 2020). Conventional
112 metrics for reporting OM and NMOG are operationally defined based on measurement methods and conditions;
113 therefore, they are difficult to compare across tests and among other ROC sources. Furthermore, uncertainties are
114 introduced when they are speciated with profiles measured at different conditions. To improve standardization, we
115 introduce two new metrics: CROC (condensable reactive organic carbon) and GROC (gaseous reactive organic
116 carbon). CROC is defined as compounds with saturation concentration (C^*) less than 320 $\mu\text{g m}^{-3}$ (Table 1), with this

117 boundary corresponding to *n*-alkanes with 20 ± 1 carbon atoms. CROC includes SVOCs ($0.32 < C^* \leq 320 \mu\text{g m}^{-3}$) and
118 low volatility organic compounds (LVOCs; $C^* \leq 0.32 \mu\text{g m}^{-3}$). Whereas, GROC is defined as the sum of compounds
119 with C^* greater than $320 \mu\text{g m}^{-3}$ corresponding to IVOCs ($320 < C^* \leq 3.2 \times 10^6 \mu\text{g m}^{-3}$) and volatile organic compounds
120 (VOCs; $C^* > 3.2 \times 10^6 \mu\text{g m}^{-3}$) (Donahue et al., 2009; Murphy et al., 2014). CROC and GROC align with well-known
121 categories in the volatility basis set (VBS) space, so they may be applied straight-forwardly to speciation profiles in
122 recent literature containing both explicit compounds and lumped groups.

123 We apply a two-step methodology to process gas- and particle-phase emissions ('ROC' path in Fig. 1). First, we
124 estimate total GROC and CROC emissions from existing NMOG and OM emission factors, respectively, while
125 considering measurement uncertainties like sampling setup losses (e.g., tubing) and filter artifacts. We then speciate
126 GROC and CROC using state-of-the-science profiles. For GROC, these include explicit IVOC compounds where
127 available and lumped IVOC groups distinguished by their saturation concentration and functionality. The
128 methodology for processing CROC emissions similarly uses volatility profiles from recent literature.

129 **2.2.1 GROC Emissions and Speciation**

130 Total NMOG emissions are measured from mobile emissions by combining total hydrocarbons (THC) with carbonyl
131 compounds and subtracting methane (see section S3) (Kishan et al., 2006; May et al., 2014). Lu et al. (2018) compiled
132 measurements for onroad vehicles, nonroad equipment, and an aircraft turbine engine. That study concluded that
133 methods using heated sampling and a heated flame-ionization detector (FID) can capture both IVOCs and VOCs, but
134 that speciation methods like canister or tedlar bag sampling analyzed with gas-chromatography-FID miss essentially
135 all IVOCs due to wall losses to the sampling materials. Assuming that NMOG emission rates are based on heated FID
136 sampling, we set GROC emission rates equal to total NMOG emission rates across all sources, and we speciated
137 GROC emissions using profiles that include VOCs and IVOCs.

138 Many studies have reported speciated organic gases normalized to total IVOC or VOC (Lu et al., 2018; Jathar et al.,
139 2017a; Zhao et al., 2015, 2016b; Huang et al., 2018; Drozd et al., 2018). A key parameter used to integrate these data
140 is the IVOC/NMOG ratio (see section S4), which ranges from ~4.6% for gasoline vehicle cold start exhaust to 67%
141 for marine residual oil. Gasoline fuel evaporation profiles of GROC were assumed to be the same as NMOG since
142 IVOCs are not expected to contribute substantially to those emissions (Gentner et al., 2012). The profile for whole
143 diesel fuel evaporation was updated to be consistent with fuel characterization in Gentner et al. (2012) (see Section
144 S1c). SPECIATEv5.1 contains thousands of explicit species and many mixtures of compounds (e.g., oils, unspeciated
145 terpenes, etc.) reported by previous studies. Recent studies have constrained the unknown portion of IVOCs and VOCs
146 with lumped groups resolved by volatility and often by structure/functionality features (e.g., branched, cyclic,
147 oxygenated, etc.). We leverage the representative compound structures in SPECIATE developed by Pye et al. (2022b)
148 to classify these emissions by functional groups, and their subsequent atmospheric chemistry. Table S2 summarizes
149 the new IVOC profiles. Species-based ozone and OA potential were calculated for each emission source using
150 relationships from Seltzer et al., (2021) which were expanded by Pye et al. (2022b)

151 2.2.2 CROC Emissions and Speciation

152 We estimate effective OM emission factors using the MOVES-predicted national total OM emissions normalized to
153 the total fuel usage for each source (see section S1). The MOVES model relies on conventional measurements of total
154 PM emissions sampled and weighed on Teflon filters. The SPECIATE database, meanwhile, stores the weight percent
155 of OC measured by thermal optical techniques from samples collected on quartz filters (U.S. Epa, 2022c) normalized
156 by coincident bulk PM measurements from the Teflon filter (see section S5). SPECIATE also applies a source-
157 dependent OM/OC factor to adjust for non-carbon organic mass (i.e. hydrogen, oxygen), which represents OM once
158 added to OC (Table S1a) (Reff et al., 2009; Simon et al., 2011). Previous studies have demonstrated that OM emission
159 factors vary with changing temperature and OM loading (Lipsky and Robinson, 2006; Robinson et al., 2010; May et
160 al., 2013a, b; Jathar et al., 2020). AQMs that take this behavior into account typically distribute OM emissions among
161 volatility bins using reference distributions. May et al. (2013a, b) constrained parameters for calculating volatility-
162 resolved emissions assuming OC is measured on a quartz filter. Although this approach performs well for average
163 cases, it is less accurate when applied to sources that are low or high emitting, for which absorptive partitioning biases
164 are more substantial (Fig. 2). For an exceedingly low-emitting source (low OM loading), SVOC emissions that would
165 normally partition to the particle phase under ambient conditions could go undetected as they pass through the filter.

166 Additionally, reported OM emissions are sometimes artifact-corrected using a secondary quartz filter behind the
167 Teflon filter sample, which allows for adsorbed SVOCs and IVOCs to be neglected. Because these corrections are not
168 uniformly applied across all studies, May et al. (2013a, b) reported reference volatility profiles assuming OM emission
169 factors had not been adsorptive-artifact corrected. Yet this is not always applicable for the emission rates informing
170 MOVES and must be resolved at the source level based on the underlying emission data. To address both adsorptive
171 and absorptive partitioning biases, we apply CROC/OM parameterizations developed from detailed measurement data
172 and informed by filter-based OM emission factors (see section S6) (May et al., 2013a, b; Huang et al., 2018; Jathar et
173 al., 2020). The method accounts for filter artifact corrections by adding missing SVOC emissions for low OM-loading
174 tests and neglecting IVOCs and higher-volatility SVOCs that would be captured on the front filter during high OM-
175 loading tests. The CROC/OM parameterization for onroad gasoline is based on data from 64 vehicles and so is more
176 robust than the parameterization for onroad heavy-duty diesel with particulate filters (DPF), which is based on 3
177 vehicles (Section S7), or the aircraft engine parameterization, which is based on one sample. These datasets show that
178 it is possible to represent the relationship between OM emission factor and CROC emission factor without explicitly
179 considering variations in temperature and OM concentration. This simplified approach is limited to mobile sources
180 because temperature is tightly controlled by test method requirements (i.e., 47 °C). Temperature is used to calculate
181 c^* of partitioning components and then calculate total CROC (e.g., Fig. S4). Because the resulting CROC emission
182 factor is highly correlated with OM emission factor, we argue that simplified functions associating them account for
183 variations due to the underlying volatility distribution and increases in concentration with emission factor. More work
184 is needed to better constrain the CROC/OM parameters.

185 The impact of this new approach for translating inventory OM emissions is shown in Fig. 2. We use the onroad
186 gasoline light-duty cold start volatility profile in Table S5 to estimate the effective ambient organic aerosol emission
187 factor at 298 K and C_{OA} equal to $10 \mu\text{g m}^{-3}$ given a filter-based OM emission factor in mg kg^{-1} fuel. Also shown are

188 trends using parameters reported by Robinson et al (2007) and Lu et al. (2020), which have been used in contemporary
189 air quality models. The filter-based OM emission factor (EF_{OM}) is multiplied by the volatility distribution, and VBS
190 partitioning theory (Eq. 1) is used to calculate the effective ambient OA emission factor ($EF_{OM,Amb}$):

$$191 \quad EF_{OM,Amb} = EF_{OM} \sum_{i=1}^{n_{tot}} \frac{\alpha_i}{1 + C_i^*/10} \quad (1)$$

192 where n_{tot} is the number of volatility parameters in the vector α . The ‘Lu et al.’ and ‘Robinson et al.’ lines are directly
193 proportional to the nonvolatile emission factor because they do not consider nonlinear dependence on the filter-based
194 OM emission factor. Meanwhile, the ROC approach enhances emissions at low emission factors (to correct for SVOC
195 breakthrough) and reduces them at high emission factors (to remove IVOCs partitioning to the filter). Also shown on
196 Fig. 2 are filter-based OM emission factors for PreTier 2, Tier 2 (2001-2004), and Tier 2 (2004+) vehicles, which
197 exhibit emissions reductions with newer standards. For the older vehicles, the ‘Lu et al.’ and ‘Robinson et al.’
198 approaches give similar estimates for effective ambient OM as the new approach, but as emission factors decrease,
199 those methods may overpredict evaporation and underpredict the particle emission factors. At the lowest OM emission
200 factors, even using the nonvolatile approach may underpredict effective ambient OA emission factors because
201 significant SVOCs could have broken through the filter and should be considered for ambient partitioning.

202 We did not adjust GROC emissions in response to CROC/OM conversion, but the sum of total ROC emissions for
203 each source does not change substantially from the sum of NMOG and OM (Fig. S22). We then updated existing
204 SPECIATE profiles with volatility distributions of LVOCs and SVOCs normalized to CROC (Table S5a). Because
205 data on the functionality of these low volatility emissions is lacking, we assume they share similar chemical properties
206 (i.e. reactivity) to linear alkanes as a proxy for more complex mixtures of aliphatics and other compounds.

207 **2.3 Air Quality Model Configuration**

208 We used an updated version of the Community Multiscale Air Quality (CMAQ) model v5.3.2 to quantify the impact
209 of the new mobile emissions on regional-scale air quality (U.S. EPA, 2021; Appel et al., 2021). Hourly ambient air
210 concentrations of OA and O₃ were simulated for the entire year 2017 at 12 km horizontal resolution with inputs from
211 EPA’s air QUALity Time Series (EQUATES) project (U.S. EPA, 2022a; Foley et al., 2023). Meteorology was
212 simulated with WRFv4.1.1. The Biogenic Emission Inventory System (BEIS) predicted biogenic gas emissions online
213 in CMAQv5.3.2. Gas- and aerosol-phase chemistry are modeled with the Carbon Bond 6 mechanism (CB6r3_AE7)
214 with updates for production of SOA from mobile IVOCs implemented by Lu et al. (2020) Anthropogenic emissions
215 are described in the US EPA 2017 emission platform technical science document and EQUATES documentation
216 (U.S. EPA, 2022b, a). Mobile emissions for 2017 were recalculated in order to update speciation and apply both
217 IVOC/NMOG and CROC/OM adjustments. The ‘CMAQ-ROC’ simulation implements all revisions to mobile
218 elemental carbon (EC) speciation described in section S2 and the methods described in sections 2.2.1 and 2.2.2. The
219 EC speciation updates result in substantial changes to nonroad diesel, aircraft, marine and rail source (Table S9).
220 Because MOVES uses source- and species-specific emission rates for HAPs rather than relying on generic speciation
221 of NMOG, ROC updates for HAPs are not propagated to the air quality model simulations, although we show potential
222 changes to national-scale HAP emissions from updates to VOC speciation. Volatile chemical product (VCP) emissions

223 are simulated for 2017 with the VCPy tool (Seltzer et al., 2021). Nonoxygenated and oxygenated IVOC emissions
224 from VCPs are represented with the IVOC chemistry from Lu et al. (2020), which results in an average SOA yield of
225 approximately 30% at ambient conditions across all IVOCs. However, Pennington et al. (2021) found the oxygenated
226 IVOC SOA yield to be 6.28%, though this yield warrants re-evaluation with better speciation and yield data given the
227 diverse mix of oxygenated IVOCs with varying molecule functionalities that can influence SOA production (Humes
228 et al., 2022). Based on available information, we reduce the CMAQ-predicted VCP SOA concentrations by 33.8% to
229 account for the overrepresentation of SOA from VCP oxygenated IVOCs (see section S7).

230 We assess model performance for O₃ and OC during the 2017 model year with daily-averaged measurements at routine
231 monitoring sites. We also perform a separate CMAQ simulation for comparison that is consistent with the EQUATES
232 project, which assumes the speciation of OM emissions from all sources are consistent with the volatility distribution
233 of a small diesel generator (Robinson et al., 2007). This ‘EQUATES’ simulation also utilizes the simplified potential-
234 combustion SOA (pcSOA) approach used in publicly available versions of CMAQ (Murphy et al., 2017). The CMAQ-
235 ROC simulation neglects pcSOA since the role of mobile and VCP IVOC SOA formation are explicitly accounted
236 for. Finally, we also analyzed two simulations with mobile and VCP SOA precursors each set to zero to quantify direct
237 sector contributions to total OA. This approach does not account for the contributions these sectors make to the
238 atmospheric oxidant capacity through emissions of low molecular weight VOCs and nitrogen oxides.

239 **3. Results and Discussion**

240 **3.1 Volatility-Resolved Mobile Source ROC Emissions**

241 Using the 2016 annual predictions from MOVES and the other mobile emission models processed and speciated with
242 the ‘ROC’ approach, we explore for the first time a complete bottom-up inventory of organic carbon emissions from
243 mobile sources in the U.S. Figure 1 shows the results of the ROC and Conventional approaches for one example
244 source, onroad heavy-duty diesel equipped with particulate filters. Non-organic particulate matter species such as ions
245 and other PM are equivalent in both approaches. Nonvolatile OM emissions in the Conventional approach are
246 distributed in the ROC approach to a range of SVOCs and IVOCs, which are predominantly alkanes and branched
247 compounds for diesel sources. The magnitude of emission factors for compounds in the VOC volatility range from
248 onroad diesel sources are reduced by 47.8% due to the introduction of IVOCs (IVOC/GROC = 52.2%), and the
249 distribution of VOC functionality is changed substantially due to adoption of VOC speciation profiles from Lu et al.
250 (2018). Unknown ROC mass is also reduced from 7% of total emissions to 0.7% after introducing IVOCs. Emission
251 factors vary by orders of magnitude across mobile sources, motivating careful accounting of sampling biases (Figs.
252 S18-S21), which requires the ROC approach in the emission modeling workflow to be complex and involve multiple
253 tools and intermediate steps (Fig. S1).

254 Figure 3 shows the predicted contributions of source types and functional groups across the volatility spectrum for
255 2016 ROC inventory. The VOC emissions are roughly evenly distributed between onroad and nonroad sources (1130
256 and 1045 kt yr⁻¹, respectively), IVOCs are weighted towards onroad (62%), and CROC (i.e. SVOCs and larger
257 compounds) is roughly split among onroad, nonroad, and others. Tailpipe (i.e. exhaust) emissions while running
258 represent the majority across all volatility categories (56% of total ROC), although evaporative sources are important

259 in the VOC range (38%), and similar to prior estimates (Gentner et al., 2009). It could be counter-intuitive, given
260 laboratory data on start and idle emission factors, that the start/idle operating mode does not contribute more to total
261 ROC emissions. This result could be due in part to substantially more time spent by sources in the running mode
262 during normal operation, but it could also be partly due to MOVES neglecting start modes for nonroad sources. Drozd
263 et al. (2018) found that cold start IVOC fuel-based emission factors are about 6 times larger than those from hot-
264 running-start emissions for newer vehicles, which is consistent with the post Tier 2 gasoline vehicles in this work. For
265 older vehicles though, the ROC inventory predicts greater IVOC emissions factors for hot-running modes than cold-
266 start for older vehicles (Table S1a and Table 2). Further research is needed to constrain NMOG emission factors and
267 IVOC/NMOG ratios for older (pre-2004) vehicles that are expected to have contributed approximately 72% of onroad
268 gasoline ROC emissions during 2017 (see Fig. S24 and Table S1a).

269 Emissions from gasoline-fueled sources dominate the VOC range in Fig. 3, but diesel-fueled sources, of which there
270 are far fewer in the U.S. dominate the IVOC range. Whereas, sources using both fuels are important for CROC
271 emissions. Mobile source VOCs comprise many functionalities, and aromatics make a substantial contribution. The
272 higher volatility IVOCs have mass associated with aromatics from gasoline sources, but cyclic hydrocarbon
273 compounds contribute to IVOCs across all volatilities, a feature reported by Zhao et al. (2015) We currently lack data
274 to specify CROC functionality across all mobile categories, so we have labeled them alkane-like based on observations
275 of motor vehicle POA emissions (Worton et al., 2014). Improved CROC speciation is needed, especially given the
276 importance of functionality to SOA formation (Lim and Ziemann, 2009; Yee et al., 2013).

277 **3.2 Impact of Filter Artifacts**

278 Transitioning from the Conventional approach to the ROC approach has implications for near-source particle
279 concentrations and prompt SOA production. Figure 4 shows the contributions of mobile categories with results using
280 approaches from previous work (Murphy et al., 2017; Lu et al., 2020). The Conventional approach assumes all OM
281 stays in the particle phase, which has been shown to lead to poor AQM performance (Murphy et al., 2017). The
282 ‘Robinson et al.’ case, which is consistent with CMAQv5.3.2, applies the volatility distribution for a small nonroad
283 diesel engine, where half the OM mass is assumed to be IVOCs adsorbed to filters and is thus volatilized. As seen in
284 Fig. 4, only 25% of the OM persists in the particle after evaporation in the ‘Robinson et al.’ approach. Lu et al. (2020)
285 applied gasoline and diesel-specific volatility profiles parameterized for emissions from in-use vehicles to the entire
286 mobile category, leading to less evaporation of OM than the ‘Robinson et al.’ approach. Lu et al. (2020) also applied
287 a conversion factor of 1.4 to all mobile gasoline-fueled sources to account for missing SVOCs.

288 In the ROC approach here, we apply source-specific adjustment factors (Table S6) and volatility profiles (Table S5)
289 and find similar results for onroad gasoline and nonroad diesel compared to Lu et al. (2020). However, onroad diesel
290 CROC emissions are increased by 60% relative to the CROC emissions from the ‘Lu et al.’ approach, driven by the
291 inclusion of missing SVOCs from clean test conditions for diesel engines with DPFs. Conventional OM emissions
292 from nonroad sources are greater than those from onroad for both gasoline- and diesel-fueled sources. Nonroad
293 gasoline emissions reduced by 36% relative to ‘Lu et al.’ where emission factors are large, and CROC/OM is much
294 less than 1.0 (Table S6), indicating the presence of IVOCs on the filter. Predicted conventional OM emissions from

295 air, rail, and marine sources are also important, and CROC emissions are slightly larger than OM. Across the mobile
296 sector, total CROC emissions increased by 12% relative to OM, and 42% of the CROC emissions are predicted to be
297 in the particle phase at 298 K and $10 \mu\text{g m}^{-3}$ organic aerosol (OA) loading.

298 **3.3 National-Scale Impact on PM, O₃ and HAPs**

299 When aggregated across all mobile sources, total ROC emissions are nearly identical between the Conventional
300 approach and ROC approach (Fig. 5). Total IVOC emissions are represent only 10.2% of total GROC due to the
301 substantial role of VOCs from gasoline sources to ROC emissions in the U.S. The spatial distribution of IVOC and
302 CROC emissions highlight the key role of cities, highways, and shipping lanes (Fig. S26). We calculate the OA
303 potential as the sum of particle-phase mass (calculated at 298 K and $10 \mu\text{g m}^{-3}$) for each species and the SOA yield of
304 the vapor-phase component of each species. Mobile source OA potential has contributions from all ROC volatility
305 classes with 6.8% from LVOCs, 25.4% from SVOCs, 19.1% from IVOCs, and 48.7% from VOCs (Fig. 5). The
306 estimated VOC OA potential is mainly driven by adjusted yields of aromatic VOCs, which are enhanced over previous
307 work due to corrections for vapor wall-losses of single-ring aromatic yields (Zhang et al., 2014). These metrics
308 possibly reflect an upper bound on VOC and IVOC contribution as they apply SOA yields to the precursor emission
309 without consideration of reaction rates, timescales, or competitive losses of precursors and intermediates to deposition.
310 Potential OA relative contributions from air, marine, and rail (12%) and onroad diesel (16%) sources play a larger
311 role in OA potential when emissions are estimated with the ROC approach, while nonroad gasoline and diesel (38%)
312 and onroad gasoline potential OA (34%) decrease (Fig. 6). While aromatic species dominate OA potential in the VOC
313 precursor range, in the IVOC range OA potential has larger contributions from cyclic alkane compounds from onroad
314 diesel sources (Fig. S23). In the LVOC range and below, the ROC approach assumes only alkane-like species;
315 improvements to the SPECIATE database and emissions modeling tools will support increased detail on compound
316 functionality when provided by future studies.

317 VOCs account for 97% of the ozone potential approximated by maximum incremental reactivity (MIR), and the total
318 ozone potential decreases by 8.9% due to the shift in mass from VOC to IVOC. The national-scale source distribution
319 of O₃ potential changes little between the Conventional and ROC approaches (Fig. 6). Ozone potential is dominated
320 by onroad and nonroad gasoline sources in the highest ROC volatility bins, driven by alkane, aromatic, and oxygenated
321 species, as expected (Fig. S23). Among onroad light duty gasoline vehicles, 72% of ROC emissions, 68% of O₃
322 potential, and 79% of OA potential are predicted to come from pre-Tier 2 vehicles, while these vehicles account for
323 19% of the fuel used in 2017 (Fig. S25). Heavy-duty diesel vehicles without particulate filters or selective catalytic
324 reduction systems contribute 87% of ROC emissions, 85% of O₃ potential, and 91% of OA potential while using 31%
325 of the fuel for the heavy-duty diesel onroad category.

326 National-scale HAP emissions changed substantially with updates in VOC speciation and introduction of IVOCs with
327 many species decreasing by nearly 20% or more including toluene (-19%), hexane (-22%), 1,3-butadiene (-34%), and
328 ethyl benzene (-29%) and others increasing substantially including formaldehyde (+22%), acrolein (+20%), and
329 acetaldehyde (+19%) (Fig. S25). These results emphasize the need for more research on HAP emission factors, but
330 we keep them constant for the CMAQ simulations to focus on OA and O₃ changes.

331 3.4 Air quality model results

332 Mobile ROC emissions were generated for the year 2017 to be comparable with the EQUATES 2017 emission inputs.
333 Differences between the EQUATES mobile inputs and those for the CMAQ-ROC simulation (Table S9) are consistent
334 with the changes in the 2016 emissions results depicted in Fig. 4. The CMAQ-ROC simulation predicts lower OC
335 concentrations throughout the domain due to elimination of pcSOA. CMAQ-ROC predictions compared well against
336 both O₃ and OC measurements at Air Quality System (AQS) sites in 2017 (Figs. S28, S29 and Table S10). Normalized
337 mean biases for OC improved (in absolute terms and on average) by 11.3% in spring, 4.3% in autumn, and 7.6% in
338 winter. In summer, the OC underprediction increased by 12%. Overprediction in the northeast, Ohio Valley, Upper
339 Midwest, and northwest in winter is consistent with timing and geography of residential wood combustion emissions,
340 which may be overrepresented in both simulations. Root mean square error and correlation coefficient differences
341 between the EQUATES and CMAQ-ROC simulations are small. CMAQ predicts both the annual mean and variability
342 of OC concentrations well at selected U.S. cities (Fig. S34, S35), with the exception of New York City where the
343 model overpredicted OC by more than a factor of 2.

344 The predicted annual population-weighted average OA attributable to mobile sources is 0.26 μg m⁻³, or 9% of the OA
345 from all anthropogenic and biogenic sources. Mobile source contributions to POA and SOA are similar on average,
346 with apparent spatial differences (Fig. 7). Average total mobile source OA appears stable between winter and summer
347 seasons (Fig. S30), and this is a result of trade-offs between higher POA concentrations in winter and higher SOA in
348 summer (Figs. S31, S32). In rural areas, model-predicted mobile OA contributions asymptote at 4.5% of total OA,
349 and in some urban areas they can exceed 23% (annual averages; Fig. S33). The ratio of SOA to OA is equal to 70%
350 in rural areas and decreases with increasing population to 20-40%. Diurnal profiles at select cities indicate SOA
351 formation peaks at noon in Los Angeles, Denver, Chicago and New York, but that feature is not reproduced on average
352 at Houston and Raleigh (Figs S34, S35).

353 CMAQ-ROC mobile and VCP IVOC concentrations are enhanced in urban areas with minimal seasonal differences
354 predicted (Figs. S36, S37). Mobile sources are predicted to contribute 20-25% to total IVOCs depending on location
355 and time of year, while VCP sources contribute 59-66% (Fig. S36), although IVOCs from other sources are
356 underrepresented. The composition of ambient IVOCs predicted by CMAQ-ROC and the speciation of IVOC
357 emissions from mobile and VCP emissions are consistent with results from Zhao et al. (Fig. S38). Since ambient
358 IVOC concentration measurements for 2017 are lacking, we extrapolated concentrations to the CalNex campaign in
359 2010 and find acceptable agreement with campaign-average hydrocarbon and oxygenated IVOC observations (section
360 S8, Fig. S39a,b). Extrapolation of CMAQ-ROC SOA to 2010 underpredicts mean CalNex SOA observations by 46%
361 (Fig. S39c,d). Potential explanations include underestimated emissions from other sources (e.g. cooking),
362 mischaracterized chemical processing (e.g. SOA yields), or errors in modeling regional pollution in Southern
363 California (Lu et al., 2020).

364 The U.S. annual GROC emission rate for mobile (2.49 Tg yr⁻¹) is 20% less than that of VCPs (3.09 Tg yr⁻¹), but the
365 mobile IVOC emissions (0.25 Tg yr⁻¹) are only one third those of VCPs (0.77 Tg yr⁻¹). Gas-phase oxidation is

366 responsible for less than half (42% and 44%) of the loss of mobile and VCP SOA-forming GROC, but 88-90% of the
367 IVOC loss (Fig. 8). The annual production and loss of total OA from mobile and VCPs is similar, and loss is distributed
368 evenly across deposition processes and transport out of the model domain. The annual rate of OA production (emission
369 plus chemical production) estimated by CMAQ and normalized to total ROC emissions (i.e. the sum of NMOG plus
370 conventional OM) is $0.16 \text{ g OA (g ROC)}^{-1}$, which is approximately equal to that estimated from the data in Fig. 5. This
371 agreement is surprising considering that the latter calculation does not account for variations in OA partitioning, NO_x
372 effects on SOA yields, or competitive losses from wet scavenging and dry deposition. Seasonal trends for OA, SOA
373 and POA production rates and ambient concentrations normalized to OM and NMOG emissions are tabulated in Table
374 S11 and discussed in section S9. These data may inform simple (e.g. screening) models of the impact of anthropogenic
375 emissions on human exposure.

376 **4. Conclusions**

377 This study implements a detailed source- and species-level procedure for converting conventional OM and NMOG
378 mobile emissions to metrics compatible with the most recent science and speciation developed for atmospheric ROC.
379 Although many AQMs have implemented online or pre-processing emission adjustments to account for these
380 phenomena, (Koo et al., 2014; Murphy et al., 2017) the procedure should be embedded within emission models and
381 databases for several reasons. Most importantly, this detailed approach considers a more diverse population of sources
382 of different ages, fuels, and control technologies that are typically averaged together before they are passed to the
383 AQM. Additionally, the new procedure enables near-explicit speciation of each emission source before mapping to
384 model species used in a particular chemical mechanism. Having a detailed speciation of major emission sources is
385 critical for assessing and revising chemical mechanisms (Pye et al., 2022b). Finally, operationalizing conversions from
386 OM to CROC and NMOG to GROC alleviates AQM users from the burden of interrogating their emissions files to
387 determine whether complex scaling operations are needed. From the broader perspective of facilitating transfer of
388 knowledge between the scientific and regulatory communities, the SPECIATE database is now capable of ingesting
389 speciation profiles with factors aligned with the most recent research studies and has enhanced flexibility to
390 accommodate future updates. Nonetheless, for model applications seeking to scale legacy emission inputs, we provide
391 updated factors normalized to several levels of source aggregation in Table S12 and discuss the uncertainty introduced
392 with this approach in section S10.

393 The 2016 ROC emissions suggest slight decreases to total O_3 formation due to reappportionment of VOC to IVOC in
394 this approach, but 2017 CMAQ-ROC predictions do not meaningfully change when evaluated at AQS sites.
395 Meanwhile, mobile IVOC emissions enhance OA formation by an additional 79 kt yr^{-1} compared to estimates from
396 the EQUATES configuration (319 kt yr^{-1}). Gaps between total OA measurements and CMAQ-ROC predictions will
397 be addressed through improved modeling of other sources of ROC (e.g., VCPs, wildfires, residential wood
398 combustion, and cooking). Within the mobile sector, results indicate substantial contributions from onroad (46%) and
399 nonroad (41%) gasoline and somewhat less from onroad (5%) and nonroad (3%) diesel air, marine, and rail sources
400 (4.7%; Fig. 6). The vast majority of ROC emissions and impacts are attributable to older (pre-Tier 2 light duty gasoline

401 and non-DPF heavy duty diesel) vehicles and nonroad gasoline engines. Onroad pollution will continue to decrease
402 as these vehicles are phased out, increasing the importance of other mobile source categories and other sources.

403 This study suggests several specific uncertainties pertaining to mobile source emissions need further laboratory and
404 field investigation. Developing complete ROC volatility distributions for specific source classes and control types is
405 critical, especially within the nonroad category where fewer experimental data were available for this study. The
406 CROC/OM factors are uncertain across all mobile sources. Ideally, IVOC and CROC emissions should be sampled
407 by a filter and a broad-spectrum adsorbent tube in series to avoid filter artifacts (Khare et al., 2019). If filter-based
408 methods alone are used to inform organic aerosol emission inventories, then reducing the uncertainty in the
409 relationship between particle emission factor and total CROC will strengthen our confidence in estimating organic
410 aerosol emissions, particularly for lower-emitting technologies. Some CROC/OM ratios derived for this work are
411 between 0.85 and 1.15, indicating a limited role for partitioning bias during source testing in those cases, but many
412 are greater than 1.30, especially the lower-emitting sources. Lastly, more research is needed to determine the extent
413 to which NMOG measurements capture IVOCs (quantified by the IVOC/NMOG or IVOC/GROC ratios). These
414 parameters are especially important to understand for older vehicles and equipment which drive historical and
415 contemporary emissions. We recommend that emissions tests specifically measure and report CROC and GROC to
416 facilitate comparison among datasets and implementation in emission models. Currently, these measurements are
417 beyond the scope of typical regulatory requirements, and future progress requires research beyond regulatory methods.

418 **ASSOCIATED CONTENT**

419 The Supporting Information is available free of charge at

420 Supporting Information 1 (SI-1): Word Document

421 Supporting Information 2 (SI-2): Excel Sheet with Tables

422 The CMAQ model source code used is available via Zenodo (<https://doi.org/10.5281/zenodo.7869142>). The functions
423 to estimate OA and O₃ potential are available at <https://github.com/USEPA/CRACMM>.

424 **ACKNOWLEDGMENT**

425 The authors gratefully acknowledge contributions from U.S. EPA staff including Kristen Foley and George Pouliot
426 who for emissions inputs and Chad Bailey, Michael Hays, and Sergey Napelenok for internal technical reviews. We
427 also acknowledge Yunliang Zhao of the California Air Resources Board for valuable insights and consultation.

428 **AUTHOR INFORMATION**

429 ***Corresponding Author:** Benjamin N. Murphy; Address: Center for Environmental Measurement and Modeling,
430 109 TW Alexander Dr., Durham, NC 27709, USA; Email: murphy.ben@epa.gov; Phone: 919-541-2291

431 **Author Contributions**

432 The manuscript was written and revised through contributions of all authors. All authors have given approval to the
433 final version of the manuscript. DS made contributions to the study primarily when employed by US EPA.

434 **DISCLAIMER**

435 *The views expressed in this article are those of the author(s) and do not necessarily represent the views or the policies*
436 *of the U.S. Environmental Protection Agency*

437 **COMPETING INTERESTS.**

438 *Some authors are members of the editorial board of ACP. The peer-review process was guided by an independent*
439 *editor, and the authors have also no other competing interests to declare.*

440 **REFERENCES**

- 441 Ahmadov, R., McKeen, S. A., Robinson, A. L., Bahreini, R., Middlebrook, A. M., de Gouw, J. A., Meagher, J.,
442 Hsie, E. Y., Edgerton, E., Shaw, S., and Trainer, M.: A volatility basis set model for summertime secondary
443 organic aerosols over the eastern united states in 2006, *J Geophys Res-Atmos*, 117, 10.1029/2011jd016831,
444 2012.
- 445 Appel, K. W., Bash, J. O., Fahey, K. M., Foley, K. M., Gilliam, R. C., Hogrefe, C., Hutzell, W. T., Kang, D.,
446 Mathur, R., Murphy, B. N., Napelenok, S. L., Nolte, C. G., Pleim, J. E., Pouliot, G. A., Pye, H. O. T., Ran,
447 L., Roselle, S. J., Sarwar, G., Schwede, D. B., Sidi, F. I., Spero, T. L., and Wong, D. C.: The community
448 multiscale air quality (cmaq) model versions 5.3 and 5.3.1: System updates and evaluation, *Geosci Model*
449 *Dev*, 14, 2867-2897, 10.5194/gmd-14-2867-2021, 2021.
- 450 Bergström, R., Denier Van Der Gon, H., Prévôt, A. S., Yttri, K. E., and Simpson, D.: Modelling of organic aerosols
451 over europe (2002–2007) using a volatility basis set (vbs) framework: Application of different assumptions
452 regarding the formation of secondary organic aerosol, *Atmospheric Chemistry and Physics*, 12, 8499-8527,
453 10.5194/acp-12-8499-2012, 2012.
- 454 Bessagnet, B., Allemand, N., Putaud, J. P., Couvidat, F., Andre, J. M., Simpson, D., Pisoni, E., Murphy, B. N., and
455 Thunis, P.: Emissions of carbonaceous particulate matter and ultrafine particles from vehicles-a scientific
456 review in a cross-cutting context of air pollution and climate change, *Appl Sci (Basel)*, 12, 1-52,
457 10.3390/app12073623, 2022.
- 458 Birch, M. and Cary, R.: Elemental carbon-based method for monitoring occupational exposures to particulate diesel
459 exhaust, *Aerosol Science and Technology*, 25, 221-241, 10.1080/02786829608965393, 1996.
- 460 Chang, X., Zhao, B., Zheng, H. T., Wang, S. X., Cai, S. Y., Guo, F. Q., Gui, P., Huang, G. H., Wu, D., Han, L. C.,
461 Xing, J., Man, H. Y., Hu, R. L., Liang, C. R., Xu, Q. C., Qiu, X. H., Ding, D., Liu, K. Y., Han, R.,
462 Robinson, A. L., and Donahue, N. M.: Full-volatility emission framework corrects missing and
463 underestimated secondary organic aerosol sources, *One Earth*, 5, 403-412, 10.1016/j.oneear.2022.03.015,
464 2022.
- 465 Chow, J. C., Watson, J. G., Pritchett, L. C., Pierson, W. R., Frazier, C. A., and Purcell, R. G.: The dri thermal/optical
466 reflectance carbon analysis system: Description, evaluation and applications in us air quality studies,
467 *Atmospheric Environment. Part A. General Topics*, 27, 1185-1201, 10.1016/0960-1686(93)90245-T, 1993.
- 468 Donahue, N. M., Robinson, A. L., and Pandis, S. N.: Atmospheric organic particulate matter: From smoke to
469 secondary organic aerosol, *Atmospheric Environment*, 43, 94-106, 10.1016/j.atmosenv.2008.09.055, 2009.
- 470 Drozd, G. T., Zhao, Y., Saliba, G., Frodin, B., Maddox, C., Oliver Chang, M.-C., Maldonado, H., Sardar, S., Weber,
471 R. J., and Robinson, A. L.: Detailed speciation of intermediate volatility and semivolatile organic
472 compound emissions from gasoline vehicles: Effects of cold-starts and implications for secondary organic
473 aerosol formation, *Environmental science & technology*, 53, 1706-1714, 10.1021/acs.est.8b05600, 2018.
- 474 FAA: Aviation environmental design tool (aedt) version 3e, U.S Department of Transportation <https://aedt.faa.gov/>,
475 2022.
- 476 Foley, K. M., Pouliot, G. A., Eyth, A., Aldridge, M. F., Allen, C., Appel, K. W., Bash, J. O., Beardsley, M., Beidler,
477 J., and Choi, D.: 2002-2017 anthropogenic emissions data for air quality modeling over the united states,
478 *Data in Brief*, 109022, 10.1016/j.dib.2023.109022, 2023.
- 479 Gentner, D. R., Harley, R. A., Miller, A. M., and Goldstein, A. H.: Diurnal and seasonal variability of gasoline-
480 related volatile organic compound emissions in riverside, california, *Environmental science & technology*,
481 43, 4247-4252, 10.1021/es9006228, 2009.
- 482 Gentner, D. R., Isaacman, G., Worton, D. R., Chan, A. W., Dallmann, T. R., Davis, L., Liu, S., Day, D. A., Russell,
483 L. M., Wilson, K. R., Weber, R., Guha, A., Harley, R. A., and Goldstein, A. H.: Elucidating secondary
484 organic aerosol from diesel and gasoline vehicles through detailed characterization of organic carbon
485 emissions, *Proc Natl Acad Sci U S A*, 109, 18318-18323, 10.1073/pnas.1212272109, 2012.

486 Gentner, D. R., Jathar, S. H., Gordon, T. D., Bahreini, R., Day, D. A., El Haddad, I., Hayes, P. L., Pieber, S. M.,
487 Platt, S. M., de Gouw, J., Goldstein, A. H., Harley, R. A., Jimenez, J. L., Prevot, A. S., and Robinson, A.
488 L.: Review of urban secondary organic aerosol formation from gasoline and diesel motor vehicle
489 emissions, *Environ Sci Technol*, 51, 1074-1093, 10.1021/acs.est.6b04509, 2017.

490 Heald, C. L. and Kroll, J. H.: The fuel of atmospheric chemistry: Toward a complete description of reactive organic
491 carbon, *Sci Adv*, 6, eaay8967, 10.1126/sciadv.aay8967, 2020.

492 Huang, C., Hu, Q., Li, Y., Tian, J., Ma, Y., Zhao, Y., Feng, J., An, J., Qiao, L., Wang, H., Jing, S., Huang, D., Lou,
493 S., Zhou, M., Zhu, S., Tao, S., and Li, L.: Intermediate volatility organic compound emissions from a large
494 cargo vessel operated under real-world conditions, *Environ Sci Technol*, 52, 12934-12942,
495 10.1021/acs.est.8b04418, 2018.

496 Humes, M. B., Wang, M., Kim, S., Machesky, J. E., Gentner, D. R., Robinson, A. L., Donahue, N. M., and Presto,
497 A. A.: Limited secondary organic aerosol production from acyclic oxygenated volatile chemical products,
498 *Environmental Science & Technology*, 56, 4806-4815, 10.1021/acs.est.1c07354, 2022.

499 Jathar, S. H., Woody, M., Pye, H. O. T., Baker, K. R., and Robinson, A. L.: Chemical transport model simulations
500 of organic aerosol in southern california: Model evaluation and gasoline and diesel source contributions,
501 *Atmos Chem Phys*, 17, 4305-4318, 10.5194/acp-17-4305-2017, 2017a.

502 Jathar, S. H., Friedman, B., Galang, A. A., Link, M. F., Brophy, P., Volckens, J., Eluri, S., and Farmer, D. K.:
503 Linking load, fuel, and emission controls to photochemical production of secondary organic aerosol from a
504 diesel engine, *Environ Sci Technol*, 51, 1377-1386, 10.1021/acs.est.6b04602, 2017b.

505 Jathar, S. H., Sharma, N., Galang, A., Vanderheyden, C., Takhar, M., Chan, A. W. H., Pierce, J. R., and Volckens,
506 J.: Measuring and modeling the primary organic aerosol volatility from a modern non-road diesel engine,
507 *Atmospheric Environment*, 223, 117221, 10.1016/j.atmosenv.2019.117221, 2020.

508 Khare, P., Marcotte, A., Sheu, R., Walsh, A. N., Ditto, J. C., and Gentner, D. R.: Advances in offline approaches for
509 trace measurements of complex organic compound mixtures via soft ionization and high-resolution tandem
510 mass spectrometry, *Journal of Chromatography A*, 1598, 163-174, 10.1016/j.chroma.2018.09.014, 2019.

511 Kishan, S., Burnette, A., FUncher, S., Sabisch, M., Crews, E., Snow, R., Zmud, M., Santos, R., Bricka, S., Fujita, E.,
512 Campbell, D., and Arnott, P.: Kansas city pm characterization study final report, 2006.

513 Koo, B., Knipping, E., and Yarwood, G.: 1.5-dimensional volatility basis set approach for modeling organic aerosol
514 in camx and cmaq, *Atmospheric Environment*, 95, 158-164, 10.1016/j.atmosenv.2014.06.031, 2014.

515 Lim, Y. B. and Ziemann, P. J.: Chemistry of secondary organic aerosol formation from oh radical-initiated reactions
516 of linear, branched, and cyclic alkanes in the presence of no x, *Aerosol Science and Technology*, 43, 604-
517 619, 10.1080/02786820902802567, 2009.

518 Lipsky, E. M. and Robinson, A. L.: Effects of dilution on fine particle mass and partitioning of semivolatile organics
519 in diesel exhaust and wood smoke, *Environ Sci Technol*, 40, 155-162, 10.1021/es050319p, 2006.

520 Lu, Q., Murphy, B. N., Qin, M., Adams, P. J., Zhao, Y., Pye, H. O. T., Efstathiou, C., Allen, C., and Robinson, A.
521 L.: Simulation of organic aerosol formation during the calnex study: Updated mobile emissions and
522 secondary organic aerosol parameterization for intermediate-volatility organic compounds, *Atmos Chem
523 Phys*, 20, 4313-4332, 10.5194/acp-20-4313-2020, 2020.

524 Lu, Q. Y., Zhao, Y. L., and Robinson, A. L.: Comprehensive organic emission profiles for gasoline, diesel, and gas-
525 turbine engines including intermediate and semi-volatile organic compound emissions, *Atmospheric
526 Chemistry and Physics*, 18, 17637-17654, 10.5194/acp-18-17637-2018, 2018.

527 Lurmann, F., Avol, E., and Gilliland, F.: Emissions reduction policies and recent trends in southern california's
528 ambient air quality, *J Air Waste Manag Assoc*, 65, 324-335, 10.1080/10962247.2014.991856, 2015.

529 Manavi, S. E. and Pandis, S. N.: A lumped species approach for the simulation of secondary organic aerosol
530 production from intermediate volatility organic compounds (ivocs): Application to road transport in
531 pmcamx-iv (v1. 0), *Geoscientific Model Development Discussions*, 1-35, 10.5194/gmd-2022-90, 2022.

532 May, A. A., Presto, A. A., Hennigan, C. J., Nguyen, N. T., Gordon, T. D., and Robinson, A. L.: Gas-particle
533 partitioning of primary organic aerosol emissions: (2) diesel vehicles, *Environ Sci Technol*, 47, 8288-8296,
534 10.1021/es400782j, 2013a.

535 May, A. A., Presto, A. A., Hennigan, C. J., Nguyen, N. T., Gordon, T. D., and Robinson, A. L.: Gas-particle
536 partitioning of primary organic aerosol emissions: (1) gasoline vehicle exhaust, *Atmospheric Environment*,
537 77, 128-139, 10.1016/j.atmosenv.2013.04.060, 2013b.

538 May, A. A., Nguyen, N. T., Presto, A. A., Gordon, T. D., Lipsky, E. M., Karve, M., Gutierrez, A., Robertson, W. H.,
539 Zhang, M., Brandow, C., Chang, O., Chen, S. Y., Cicero-Fernandez, P., Dinkins, L., Fuentes, M., Huang,
540 S. M., Ling, R., Long, J., Maddox, C., Massetti, J., McCauley, E., Miguel, A., Na, K., Ong, R., Pang, Y. B.,
541 Rieger, P., Sax, T., Truong, T., Vo, T., Chattopadhyay, S., Maldonado, H., Maricq, M. M., and Robinson,

542 A. L.: Gas- and particle-phase primary emissions from in-use, on-road gasoline and diesel vehicles,
 543 Atmospheric Environment, 88, 247-260, 10.1016/j.atmosenv.2014.01.046, 2014.
 544 Morino, Y., Chatani, S., Fujitani, Y., Tanabe, K., Murphy, B. N., Jathar, S. H., Takahashi, K., Sato, K., Kumagai,
 545 K., and Saito, S.: Emissions of condensable organic aerosols from stationary combustion sources over
 546 Japan, Atmospheric Environment, 289, 119319, 10.1016/j.atmosenv.2022.119319, 2022.
 547 Murphy, B. N. and Pandis, S. N.: Simulating the formation of semivolatile primary and secondary organic aerosol in
 548 a regional chemical transport model, Environ Sci Technol, 43, 4722-4728, 10.1021/es803168a, 2009.
 549 Murphy, B. N., Donahue, N. M., Robinson, A. L., and Pandis, S. N.: A naming convention for atmospheric organic
 550 aerosol, Atmospheric Chemistry and Physics, 14, 5825-5839, 10.5194/acp-14-5825-2014, 2014.
 551 Murphy, B. N., Woody, M. C., Jimenez, J. L., Carlton, A. M. G., Hayes, P. L., Liu, S., Ng, N. L., Russell, L. M.,
 552 Setyan, A., Xu, L., Young, J., Zaveri, R. A., Zhang, Q., and Pye, H. O. T.: Semivolatile poa and
 553 parameterized total combustion soa in cmaq5.2: Impacts on source strength and partitioning, Atmos Chem
 554 Phys, 17, 11107-11133, 10.5194/acp-17-11107-2017, 2017.
 555 Pennington, E. A., Seltzer, K. M., Murphy, B. N., Qin, M., Seinfeld, J. H., and Pye, H. O.: Modeling secondary
 556 organic aerosol formation from volatile chemical products, Atmospheric chemistry and physics, 21, 18247-
 557 18261, 10.5194/acp-21-18247-2021, 2021.
 558 Pye, H. O. T., Appel, K. W., Seltzer, K. M., Ward-Caviness, C. K., and Murphy, B. N.: Human-health impacts of
 559 controlling secondary air pollution precursors, Environ Sci Technol Lett, 9, 96-101,
 560 10.1021/acs.estlett.1c00798, 2022a.
 561 Pye, H. O. T., Place, B. K., Murphy, B. N., Seltzer, K. M., and D'Ambro, E. L.: Linking gas, particulate, and toxic
 562 endpoints to air emissions in the community regional atmospheric chemistry multiphase mechanism
 563 (cracmm) version 1.0 Atmospheric Chemistry and Physics, 2022b.
 564 Pye, H. O. T., Ward-Caviness, C. K., Murphy, B. N., Appel, K. W., and Seltzer, K. M.: Secondary organic aerosol
 565 association with cardiorespiratory disease mortality in the United States, Nat Commun, 12, 7215,
 566 10.1038/s41467-021-27484-1, 2021.
 567 Reff, A., Bhavsar, P. V., Simon, H., Pace, T. G., Pouliot, G. A., Mobley, J. D., and Houyoux, M.: Emissions inventory
 568 of pm2.5 trace elements across the United States, Environ Sci Technol, 43, 5790-5796, 10.1021/es802930x,
 569 2009.
 570 Robinson, A. L., Grieshop, A. P., Donahue, N. M., and Hunt, S. W.: Updating the conceptual model for fine particle
 571 mass emissions from combustion systems. A. L. Robinson, Journal of the Air & Waste Management
 572 Association, 60, 1204-1222, 10.3155/1047-3289.60.10.1204, 2010.
 573 Robinson, A. L., Donahue, N. M., Shrivastava, M. K., Weitkamp, E. A., Sage, A. M., Grieshop, A. P., Lane, T. E.,
 574 Pierce, J. R., and Pandis, S. N.: Rethinking organic aerosols: Semivolatile emissions and photochemical
 575 aging, Science, 315, 1259-1262, 10.1126/science.1133061, 2007.
 576 Safieddine, S. A., Heald, C. L., and Henderson, B. H.: The global nonmethane reactive organic carbon budget: A
 577 modeling perspective, Geophysical Research Letters, 44, 3897-3906, 10.1002/2017gl072602, 2017.
 578 Sarica, T., Sartelet, K., Roustan, Y., Kim, Y., Lugon, L., Marques, B., D'Anna, B., Chaillou, C., and Larrieu, C.:
 579 Sensitivity of pollutant concentrations in urban streets to asphalt and traffic-related emissions,
 580 Environmental Pollution, 121955, 10.1016/j.envpol.2023.121955, 2023.
 581 Seltzer, K. M., Pennington, E., Rao, V., Murphy, B. N., Strum, M., Isaacs, K. K., and Pye, H. O. T.: Reactive
 582 organic carbon emissions from volatile chemical products, Atmos Chem Phys, 21, 5079-5100,
 583 10.5194/acp-21-5079-2021, 2021.
 584 Shrivastava, M., Fast, J., Easter, R., Gustafson, W. I., Zaveri, R. A., Jimenez, J. L., Saide, P., and Hodzic, A.:
 585 Modeling organic aerosols in a megacity: Comparison of simple and complex representations of the
 586 volatility basis set approach, Atmospheric Chemistry and Physics, 11, 6639-6662, 10.5194/acp-11-6639-
 587 2011, 2011.
 588 Simon, H., Bhavsar, P. V., Swall, J. L., Frank, N. H., and Malm, W. C.: Determining the spatial and seasonal
 589 variability in om/oc ratios across the US using multiple regression, Atmospheric Chemistry and Physics, 11,
 590 2933-2949, 10.5194/acp-11-2933-2011, 2011.
 591 Tessum, C. W., Paoletta, D. A., Chambliss, S. E., Apte, J. S., Hill, J. D., and Marshall, J. D.: Pm2.5 pollutants
 592 disproportionately and systemically affect people of color in the United States, Sci Adv, 7, eabf4491,
 593 10.1126/sciadv.abf4491, 2021.
 594 Tkacik, D. S., Presto, A. A., Donahue, N. M., and Robinson, A. L.: Secondary organic aerosol formation from
 595 intermediate-volatility organic compounds: Cyclic, linear, and branched alkanes, Environ Sci Technol, 46,
 596 8773-8781, 10.1021/es301112c, 2012.

597 Turpin, B. J., Huntzicker, J. J., and Hering, S. V.: Investigation of organic aerosol sampling artifacts in the los-
598 angeles basin, *Atmospheric Environment*, 28, 3061-3071, 10.1016/1352-2310(94)00133-6, 1994.
599 U.S. EPA: Integrated science assessment (isa) for particulate matter (final report, dec 2019), 2019.
600 U.S. EPA: Speciatev5.1, U.S. EPA <https://www.epa.gov/air-emissions-modeling/speciate>, 2020a.
601 U.S. EPA: Motor vehicle emission simulator: Moves3, Office of Transportation and Air Quality, U.S. EPA
602 <https://www.epa.gov/moves>, 2020b.
603 U.S. EPA: Integrated science assessment (isa) for ozone and related photochemical oxidants (final report, apr 2020),
604 2020c.
605 U.S. EPA: Community multiscale air quality (cmaq) model v5.3.2, Office of Research and Development, U.S. EPA
606 <https://github.com/USEPA/CMAQ/tree/5.3.2>, 2021.
607 U.S. EPA: Equates: Epa's air quality time series project, U.S. EPA [dataset], 2022a.
608 U.S. EPA: Technical support document (tsd) preparation of emissions inventories for the 2017 north american
609 emissions modeling platform, 2022b.
610 U.S. EPA: Engine testing procedures. Cfr, part 1065, title 40, 2022c.
611 Winkler, S., Anderson, J., Garza, L., Ruona, W., Vogt, R., and Wallington, T.: Vehicle criteria pollutant (pm, nox,
612 co, hcs) emissions: How low should we go?, *Npj Climate and atmospheric science*, 1, 1-5, 10.1038/s41612-
613 018-0037-5, 2018.
614 Woody, M. C., West, J. J., Jathar, S. H., Robinson, A. L., and Arunachalam, S.: Estimates of non-traditional
615 secondary organic aerosols from aircraft svoc and ivoc emissions using cmaq, *Atmospheric Chemistry and
616 Physics*, 15, 6929-6942, 10.5194/acp-15-6929-2015, 2015.
617 Woody, M. C., Baker, K. R., Hayes, P. L., Jimenez, J. L., Koo, B., and Pye, H. O.: Understanding sources of organic
618 aerosol during calnex-2010 using the cmaq-vbs, *Atmospheric Chemistry and Physics*, 16, 4081-4100,
619 10.5194/acp-16-4081-2016, 2016.
620 Worton, D. R., Isaacman, G., Gentner, D. R., Dallmann, T. R., Chan, A. W., Ruehl, C., Kirchstetter, T. W., Wilson,
621 K. R., Harley, R. A., and Goldstein, A. H.: Lubricating oil dominates primary organic aerosol emissions
622 from motor vehicles, *Environmental science & technology*, 48, 3698-3706, 10.1021/es405375j, 2014.
623 Yee, L., Craven, J., Loza, C., Schilling, K., Ng, N., Canagaratna, M., Ziemann, P., Flagan, R., and Seinfeld, J.:
624 Effect of chemical structure on secondary organic aerosol formation from c 12 alkanes, *Atmospheric
625 Chemistry and Physics*, 13, 11121-11140, 10.5194/acp-13-11121-2013, 2013.
626 Zhang, X., Cappa, C. D., Jathar, S. H., McVay, R. C., Ensberg, J. J., Kleeman, M. J., and Seinfeld, J. H.: Influence
627 of vapor wall loss in laboratory chambers on yields of secondary organic aerosol, *Proceedings of the
628 National Academy of Sciences*, 111, 5802-5807, 10.1073/pnas.1404727111, 2014.
629 Zhao, B., Wang, S., Donahue, N. M., Jathar, S. H., Huang, X., Wu, W., Hao, J., and Robinson, A. L.: Quantifying
630 the effect of organic aerosol aging and intermediate-volatility emissions on regional-scale aerosol pollution
631 in china, *Sci Rep*, 6, 28815, 10.1038/srep28815, 2016a.
632 Zhao, Y., Tkacik, D. S., May, A. A., Donahue, N. M., and Robinson, A. L.: Mobile sources are still an important
633 source of secondary organic aerosol and fine particulate matter in the los angeles region, *Environmental
634 Science & Technology*, 56, 15328-15336, 10.1021/acs.est.2c03317, 2022.
635 Zhao, Y., Nguyen, N. T., Presto, A. A., Hennigan, C. J., May, A. A., and Robinson, A. L.: Intermediate volatility
636 organic compound emissions from on-road diesel vehicles: Chemical composition, emission factors, and
637 estimated secondary organic aerosol production, *Environ Sci Technol*, 49, 11516-11526,
638 10.1021/acs.est.5b02841, 2015.
639 Zhao, Y., Nguyen, N. T., Presto, A. A., Hennigan, C. J., May, A. A., and Robinson, A. L.: Intermediate volatility
640 organic compound emissions from on-road gasoline vehicles and small off-road gasoline engines, *Environ
641 Sci Technol*, 50, 4554-4563, 10.1021/acs.est.5b06247, 2016b.
642 Zhao, Y., Hennigan, C. J., May, A. A., Tkacik, D. S., de Gouw, J. A., Gilman, J. B., Kuster, W. C., Borbon, A., and
643 Robinson, A. L.: Intermediate-volatility organic compounds: A large source of secondary organic aerosol,
644 *Environ Sci Technol*, 48, 13743-13750, 10.1021/es5035188, 2014.

645

646

647

648

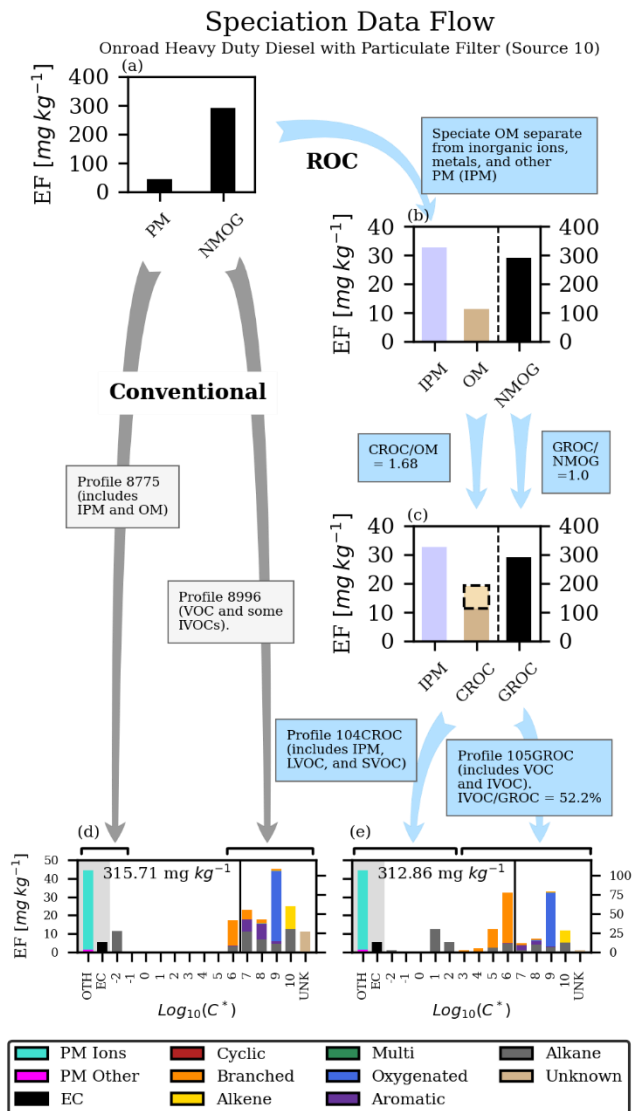
649

Table 1. Definitions of key terms.

Acronym	Definition
OM	Organic matter component of primary particle emissions as measured on a filter.
NMOG	Non-methane organic gas emissions
POA	Primary organic aerosol. Particle-phase emissions after equilibrium is reached with ambient conditions.
OA	Particle-phase organic material at ambient conditions.
LVOC	Low-volatility organic compounds ($C^* \leq 0.32 \mu\text{g m}^{-3}$).
SVOC	Semivolatile organic compounds ($0.32 < C^* \leq 320 \mu\text{g m}^{-3}$).
IVOC	Intermediate volatility organic compounds ($320 < C^* \leq 3.2 \times 10^6 \mu\text{g m}^{-3}$).
VOC	Volatile organic compounds ($3.2 \times 10^6 \mu\text{g m}^{-3} < C^*$).
CROC	Condensable reactive organic carbon: particle- and gas-phase LVOC + SVOC. Carbon and noncarbon mass are included.
GROC	Gaseous reactive organic carbon: particle- and gas-phase IVOC + VOC. Carbon and noncarbon mass are included.
ROC	Reactive organic carbon – all particle and gas organic compounds mass except methane. Carbon and noncarbon mass are included.

650

651



652

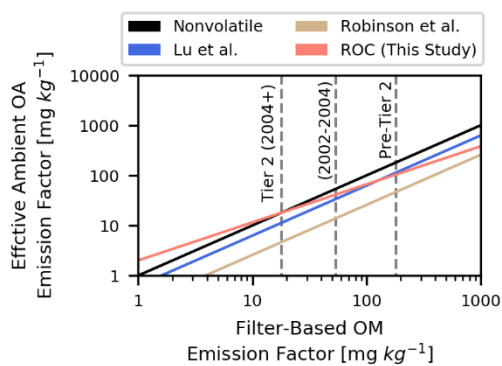
653 **Figure 1.** Depiction of calculation steps for the Conventional and ROC approaches to speciation of PM and NMOG
 654 emissions. Panel (a) shows the reported fuel-based emission factors based on MOVES predictions for 2016. Panel
 655 (b) shows the inorganic ions, metals and other nonorganic matter (IPM) separated from organic matter (OM). The
 656 beige area inside the dashed box in panel (c) indicates emissions that are added in the conversion of OM to CROC to
 657 account for underrepresented SVOCs from the filter measurement. Panels (d) and (e) show the comprehensive
 658 emission factors for the Conventional and ROC approaches, respectively, with data arranged by volatility while
 659 indicating non-organic PM emissions as well. In panels (d) and (e), bars to the left and right of the vertical line at
 660 $\text{Log}_{10}(C^*) = 6.5$ are quantified by the left and right y axes, respectively. The number within panels (d) and (e)
 661 indicates the total ROC emission factor excluding EC and Other PM for onroad heavy-duty diesel sources. ‘Alkane’
 662 refers to only linear alkanes, while ‘cyclic’ and ‘branched’ are cyclic alkanes and branched alkanes. ‘Multi’

663 indicates multifunctional organics. The bars in the gray shaded regions are not included in the organic volatility
664 distribution but are included in the CROC-compatible SPECIATE profiles (e.g. 104CROC).

665

666

667

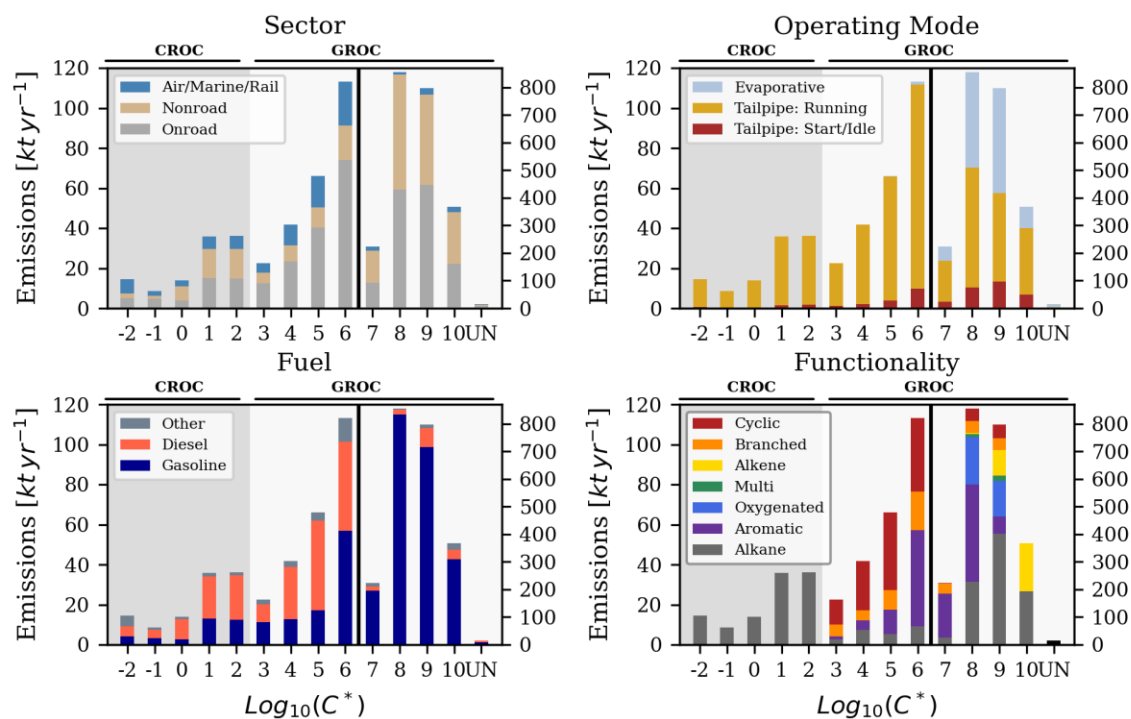


668

669 **Figure 2.** Effective ambient primary organic aerosol emission factor estimated at 298 K and $10 \mu\text{g m}^{-3}$ as a function
670 of the OM emission factor for onroad gasoline-fueled vehicles.

671

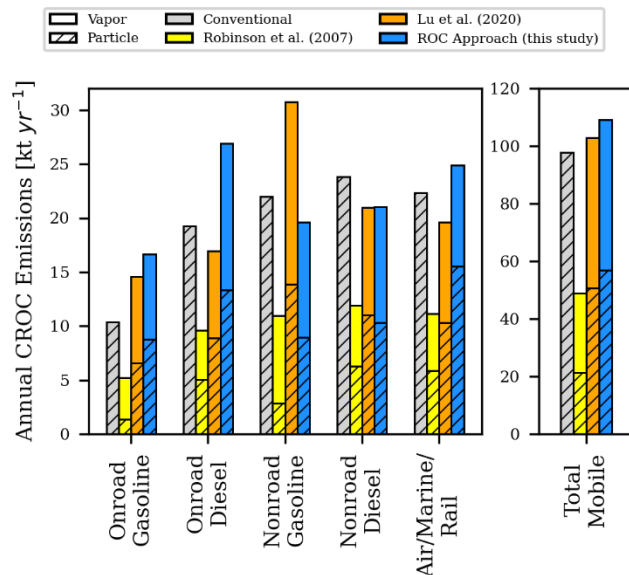
672



673

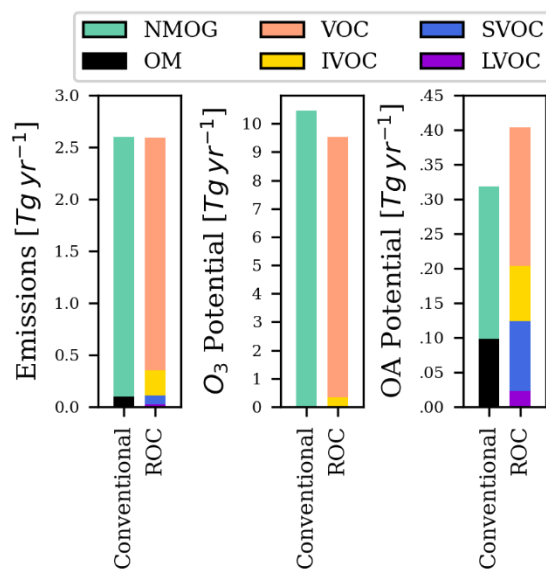
674 **Figure 3.** Volatility-resolved mobile source ROC emissions for the contiguous U.S. during 2016 stratified along
 675 several dimensions including category (top-left), operating mode (top-right), fuel (bottom-left), and chemical
 676 functionality (bottom-right). The ‘multi’ functionality series corresponds to compounds that are both oxygenated and
 677 have double carbon bonds. Bins to the left of the solid black line are quantified by the left y axis and those to the right
 678 by the right y axis. The unknown emissions (UN) are not assigned to a volatility bin and do not contribute to OA or
 679 O₃ formation.

680



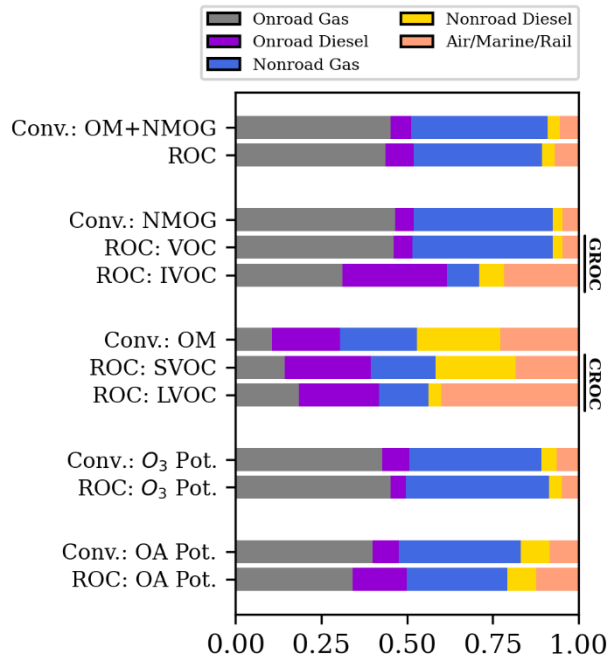
681
 682 **Figure 4.** Bottom-up predictions of 2016 annual mobile CROC (i.e. SVOC, LVOC, and lower volatility compound)
 683 emissions classified by category, model approach, and equilibrium phase distribution. The full height of each bar
 684 corresponds to total CROC emissions. Gas-particle partitioning is calculated for atmospherically relevant conditions
 685 at 298 K and organic aerosol loading of $10 \mu\text{g m}^{-3}$.

686
 687
 688

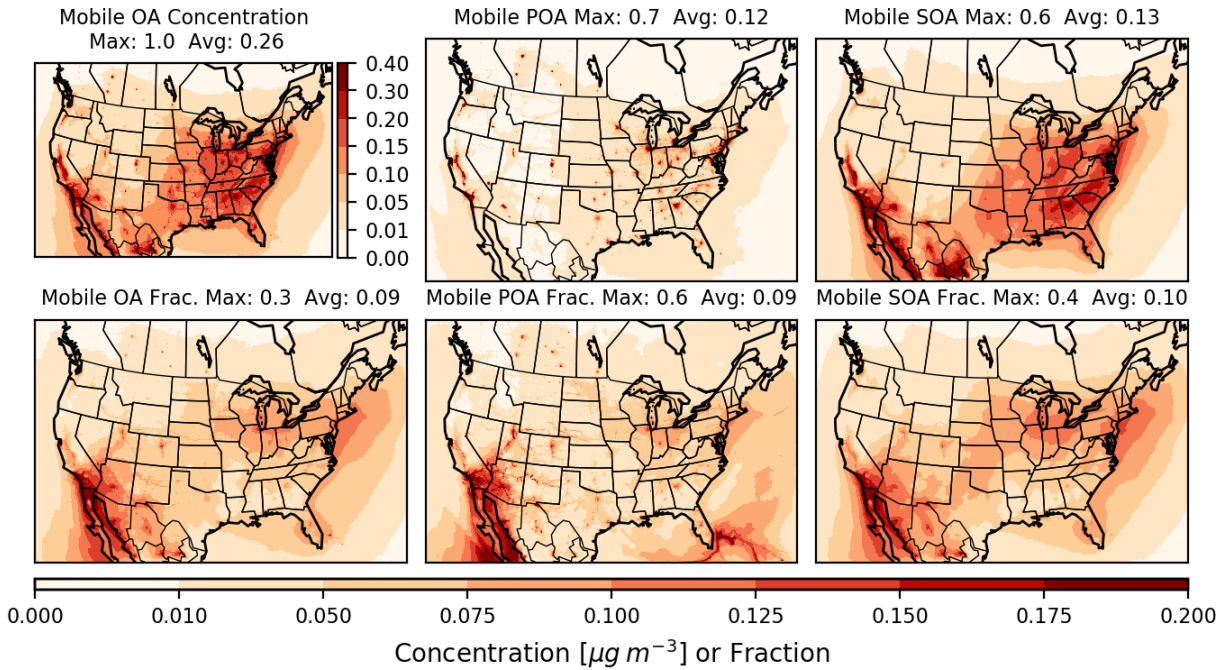


689
 690 **Figure 5.** Total U. S. mobile source emissions for 2016 with aggregate O_3 and OA potential calculated at the species
 691 level.

692

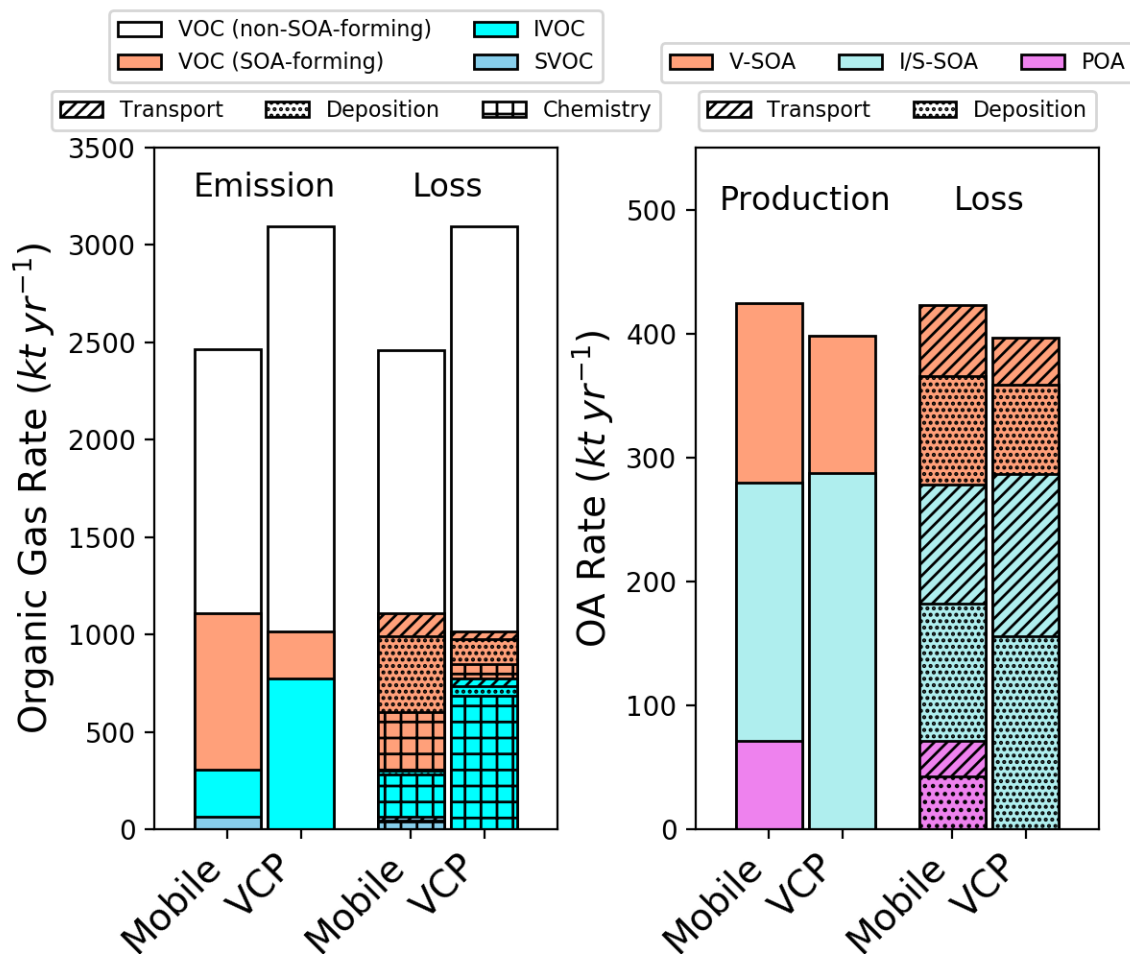


693
 694 **Figure 6.** Mobile sector contributions to ROC classes and derived quantities like O₃ and OA potential. Values are
 695 presented for the Conventional and ROC-based approaches.



696

697 **Figure 7.** Annual average concentration (top row) of total OA (left), POA (center), and SOA (right) from mobile
 698 sources predicted by CMAQ for 2017 with the ROC mobile emission inventory. The fractional contribution of mobile
 699 sources to the total of each pollutant category from all sources are on the bottom row. In all panel subtitles, ‘Max’
 700 refers to the spatial maximum of the annual average spatial field, while ‘Avg’ refers to the population-weighted
 701 average of the annual average spatial field.



702
703
704
705
706
707
708
709

Figure 8. Domain-wide predicted budget of (left) mobile and volatile chemical product (VCP) gas-phase emissions and loss due to chemistry, deposition, or transport and (right) OA production and losses for 2017. In the left plot, loss terms are only depicted for categories of compounds that lead to organic particle formation.